Journal of Nano- and Electronic Physics
Vol. **15** No 1, 01008(6pp) (2023)

Журнал нано- та електронної фізики
Том **15** № 1, 01008(6cc) (2023)

High-Performance Two-Dimensional Photonic Crystal Biosensor to Diagnose Malaria Infected RBCs

H. Tayoub[1,2,*], A. Hocini[1,†], A. Harhouz[1,‡]

[1] *Laboratoire d'Analyse des Signaux et Systèmes, Department of Electronics, University of M'Sila BP.166, Route Ichebilia, 28000 M'Sila, Algeria*
[2] *Research Center in Industrial Technologies CRTI, P.O.BOX :64, Cheraga, 16014 Algiers, Algeria*

(Received 05 January 2023; revised manuscript received 16 February 2023; published online 24 February 2023)

In this paper, a two-dimensional photonic crystal refractive index biosensor based on a ring-shaped cavity has been proposed. It is designed for the diagnosis of malaria-infected red blood cells (RBCs) in the wavelength range of 1130-1860 nm for TM-polarized light. The proposed biosensor consists of two waveguides coupled with one ring-shaped microcavity, which is obtained by removing seven lattice holes, the microcavity is separated from the two waveguides by three holes. The infiltration of the analyte into the ring-shaped cavity changes its refractive index, and this variation of the refractive index of infected and normal uninfected RBCs causes a corresponding wavelength shift at the output terminal. Consequently, a high sensitivity of more than 700 nm/RIU, an ultra-high-quality factor (Q-factor) of up to 10^6 giving a sensor figure of merit (FOM) of up to 10^6 RIU^{-1}, and a low detection limit of 10^{-7} RIU can be achieved for the proposed design. The proposed device has also an ultra-compact size of 9.78 × 8.84 μm^2 that makes it so attractive for lab-on-a-chip applications. The obtained results have demonstrated that the ring-shaped holes configuration provides an excellent optical confinement within the cavity region. The proposed design is simulated using Plane Wave Expansion (PWE) method and Finite-Difference Time-Domain (FDTD) algorithm.

Keywords: Photonic crystal, Ring-shaped cavity, Biosensor, Malaria, Sensitivity, Quality factor.

DOI: 10.21272/jnep.15(1).01008 PACS numbers: 07.07.Df, 42.79.Pw

1. INTRODUCTION

Malaria is caused by intraerythrocytic Plasmodium parasites, while there are four species of Plasmodium can infect humans [1], the species Plasmodium falciparum is the most pathogenic form of malaria with the highest number of deaths worldwide (P. falciparum accounted for 99.7 % of estimated malaria cases in the African region) [2], malaria is transmitted through the bites of infected female Anopheles mosquitoes that attack red blood and liver cells [3]. By April 2020, the severe acute respiratory syndrome coronavirus 2 (SARS-CoV2), which causes COVID-19, had spread to all malaria-endemic countries [4]. In addition, the immune response and symptoms of COVID-19, including fever or chills, cough, difficulty breathing, headache, nausea or vomiting, diarrhea, fatigue, and gastrointestinal issues are very similar to those of malaria infection. As a consequence, the diagnosis of malaria disease may be delayed [3]. Classical analytical techniques are widely used for malaria diagnosis. However, most of these methods have disadvantages, such as multi-step analysis, time-consuming, expensive analysis equipment and skilled operators, lack of on-site applicability, and hence not effective in detection and controlling the spread of the disease. Therefore, there is a need for highly sensitive, fast, simple, field-applicable, and low-cost diagnostic sensors for the diagnosis of malaria. Biosensors are detection tools that sense specific analyte using specific biological receptors molecules [5, 6], photonic crystal (PhC) biosensors play a key role in malaria diagnosis, they have recently attracted much interest because of their strong light-matter interaction between resonant modes and target analytes, which increases detection sensitivity, and because of their ease of fabrication and CMOS compatibility [7, 8]. The performance of these biosensors is evaluated by the capability to sense the smallest variation of the refractive index.

In most cases, as a result of malaria infection, red blood cells (RBCs) degenerate, and the characteristics of RBC structure change into three stages: first, the ring stage lasting 24 hours, and then the trophozoites stage within 24-36 hours. Finally, the schizont stage within 36-48 hours, according to these stages, the refractive index of each stage is 1.395, 1.383, and 1.373 [9], respectively. Therefore, the refractive index varies from normal to infected RBCs. Different sensitive biosensors for malaria diagnosis were discussed, Sharma et al. [10] proposed a 2D-PhC biosensor using red blood cells as an analyte. The sample was trapped into the nanocavity and a shift in the transmitted peak is observed. 2D-PhC ring resonator-based biosensor was presented by Bendib et al. [11] at 2.07 μm. Another version of a one-dimensional photonic crystal with a defect biosensor for malaria diagnosis at an early stage was described by Ankita et al. [12]. Moreover, M.T. Tammam et al. [13] were proposed a GaN and porous GaN-based 1D defective PhC as an optical sensor to detect malaria disease, where red blood cells samples were used as a sample defect.

In the present work, an ultra-compact 2D-PhC bio-

* hadjira.tayoub@univ-msila.dz
† abdesselam.hocini@univ-msila.dz
‡ ahlam.harhouz@univ-msila.dz

sensor that uses a ring-shaped hole as a microcavity is designed, and good sensing characteristics such as the sensitivity, Q-factor, FOM, detection limit, resonant wavelength, and normalized transmission are estimated for the three stages of malaria in the human body for the proposed biosensor compared with the reported 2D-PhC devices. The proposed high-performance PhC biosensor can be used as a valuable diagnostic tool for malaria detection at an early stage, it has a simple structure, an ultra-compact size, and high confinement of light within the microcavity region. All the simulations are done using Plane Wave Expansion (PWE) method and Finite-Difference Time-Domain (FDTD) tool of RSoft Photonic Suite CAD.

2. STRUCTURE DESIGN

In this work, the proposed structure is constructed in a silicon-on-insulator (SOI) substrate because of the strong light-matter interaction. The size of the used photonic crystal structure is (21×19), the structure design is presented as shown in Fig. 1a. It consists of a 2D hexagonal lattice of air where the radius of the air holes $r = 0.19$ μm and the air holes assumed to have an infinite length in the z-direction. The lattice constant (a) is considered as 0.47 μm, and the index profile of Si slab $n_{si} = 3.42$. The photonic bandgap (PBG) ranges from $\omega_1 = 0.25275$ (a/λ) to $\omega_2 = 0.41601$ (a/λ) (Fig. 1b) and the designed photonic crystal structure has a large bandgap in the wavelength range of 1130-1860 nm for TM-polarized light.

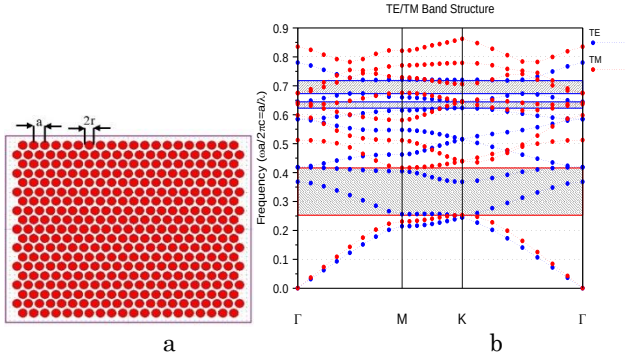

Fig. 1 – Schematic of the proposed 2D-PhC structure (a), band diagram of the proposed 2D-PhC structure (b)

3. DESIGN OF PHOTONIC CRYSTAL BIOSENSOR

For the propagation of light inside the structure, the center free space wavelength used is 1550 nm as this wavelength is suitable and well-known for biosensing purposes. To break the periodicity of the structure and localize the light, two photonic crystal waveguides W1 are created by removing one row of air holes in the ΓK direction, and a ring-shaped defect was introduced into the center of the structure by removing seven lattice holes, to form one ring-shaped cavity, and by separating the ring-shaped cavity and the two waveguides by three holes to generate localized optical modes that resonate in this ring [14] (Fig. 2). We performed 2D-PWE and 2D-FDTD simulations to study and optimize our device performance using RSoft Photonic Suite CAD. PWE is often used effectively to calculate the photonic bandgaps for two-dimensional photonic crystals, which prohibit the propagation of light at certain frequency intervals. Moreover, FDTD method is widely used to efficiently simulate the interaction of light with materials and optical devices, it is used for the numerical simulations to solve the Maxwell equations. These simulation methods are known for their several merits, including that they give an extraordinary match between simulation and fabricated results.

4. RESULTS AND DISCUSSION

4.1 The First Proposed Design (Design A)

The proposed configuration of the first design (Design A) with all the relevant geometry parameters for refractive index detection is shown in Fig. 2, the inner and outer radius of the ring-shaped hole are denoted as $R_{in} = 0.23$ and $R_{out} = 1.2a$, respectively. In the simulation process, the Gaussian light source under normal incidence with TM-polarized is placed at the input of W1 waveguide, and the power monitor is located at the end of the output W1 waveguide to obtain the transmission spectra data. The schematic of the zoomed cavity region is shown in Fig. 2b. It is noteworthy to mention that the proposed biosensor may sense all three stages of malaria as will be shown.

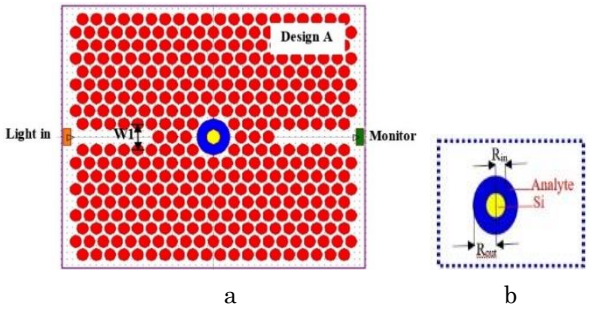

Fig. 2 – Schematic of the first proposed 2D-PhC biosensor (a), zoom of cavity region (b)

The electric field distribution is a principal parameter in fluid sensing measurement. To minimize the amount of RBCs needed for effective sensing, it is necessary to find a minimum region, which should be basically covered by blood samples [15], as shown in Fig. 3a. The electric field distribution at the resonance is mainly localized in the ring-shaped cavity and shows its maximum value at its center (Fig. 3b), which means that this region is the most sensitive to the change of refractive index due to the large degree of light-matter interaction inside it. Thus, all the presented results hereafter have been obtained by covering the ring-shaped cavity and the adjacent area by the analyte (The RBCs sample should be processed before it is analyzed [9]). The simulation of the electric field distribution was realized using PWE method.

Many approaches are using for malaria diagnosis and detection, which include microscopic diagnosis, quantitative buffy coat (QBC) method, indirect fluorescent antibody (IFA), and rapid diagnostic tests (RDT). As mentioned before, these methods have limits [16]. Detecting the refractive index of the RBCs is consid-

ered the key factor for the detection of malaria [11, 17] as the three stages of malaria infection cause a change in the refractive index of the infected RBCs. The database used in the paper is given in Table 1, the refractive index values of normal and infected RBCs are taken at a wavelength of 1550 nm.

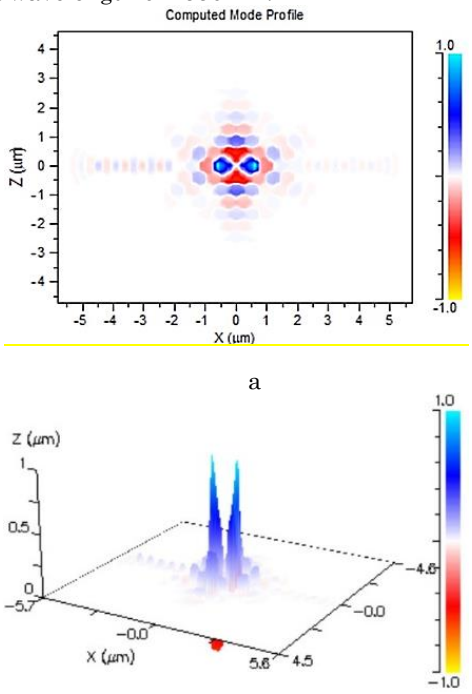

Fig. 3 – Electric field distribution at the resonance ($\lambda = 1.74414$) (a), equivalent $|E|^2$ distribution (b)

Table 1 – Refractive index values of normal and infected RBCs [9]

Name	Refractive index
Schizont phase cells	1.373
Trophozoites phase cells	1.383
Ring phase cells	1.395
Normal uninfected RBCs	1.402

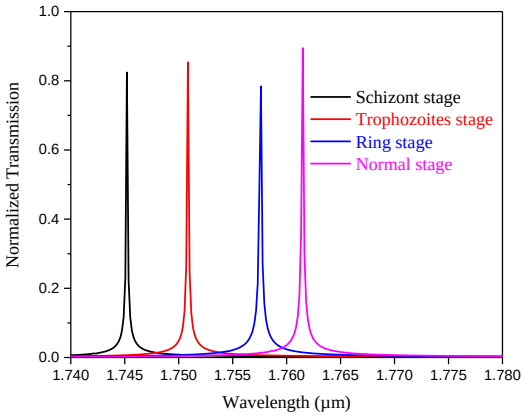

Fig. 4 – Normalized transmission spectrum for the first proposed design at optimized parameters $R_{in} = 0.23$ and $R_{out} = 1.2a$

Fig. 4 depicts the normalized transmission spectrum of the first design at the optimized parameters $R_{in} = 0.23$ and $R_{out} = 1.2a$. The transmission spectra are obtained for the normal and three stages of malaria. As can be seen, the shift in the resonant peak toward the right as a function of the change in the refractive index of the analyte, these resonant peaks occur at 1.7452 µm for schizont stage ($n = 1.373$), 1.75085 µm for trophozoite stage ($n = 1.383$), 1.75762 µm for ring stage ($n = 1.395$), and 1.76149 µm for normal stage ($n = 1.402$). As a result, the biosensor shows a high sensitivity up to 500 nm/RIU.

In order to investigate the performance of the proposed biosensor, we fixed the value of the outer radius R_{out} at 1.2a and the inner radius R_{in} is varied from 0.19 to 0.27 with a step of 0.02. The variation of the sensitivity and the resonant wavelength as a function of the inner radius R_{in} change for normal and infected RBCs are simulated as shown in Fig. 5. It can be seen quite clearly that the sensitivity reaches its maxima for $R_{in} = 0.23$ (Fig. 5a), increasing R_{in} means decreasing the sensing region due to the infiltration only within the ring-shaped cavity (the hole colored in blue in Fig. 2). Consequently, when R_{in} is more than 0.23, the sensitivity decreases because of the optical leakages. It can be noticed also that on increasing the inner radius R_{in}, the resonant wavelength values show an ascending trend up (Fig. 5b) due to the augmentation of high dielectric material in the ring-shaped cavity area [18].

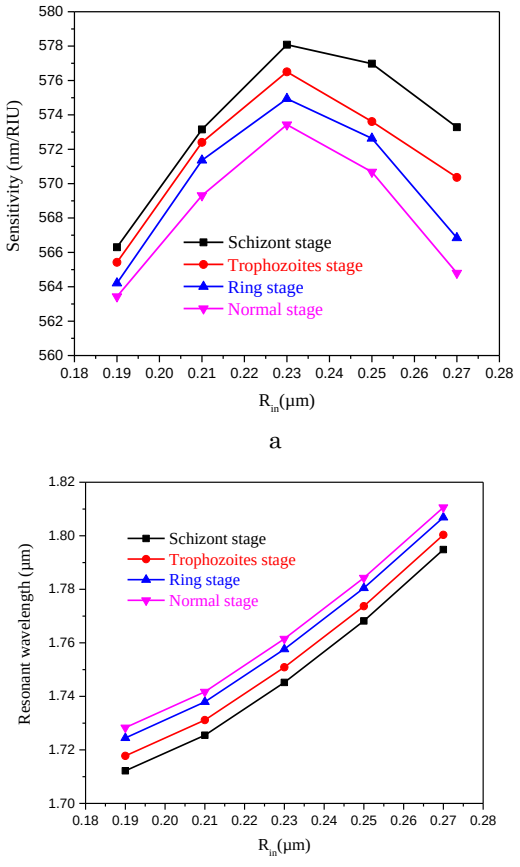

Fig. 5 – The variation of the sensitivity (a), and the resonant wavelength according to the radius of the inner ring R_{in} (b)

4.2 The Second Proposed Design (Design B)

To improve the performance of our device by adjusting the number of functionalized holes, two designs have been proposed (Designs B and C). The second proposed design (Design B) is depicted in Fig. 6, this proposed biosensor is obtained by increasing the region covered by the RBCs from the ring-shaped cavity to the twelve surrounding holes (the blue region is filled by a blood sample).

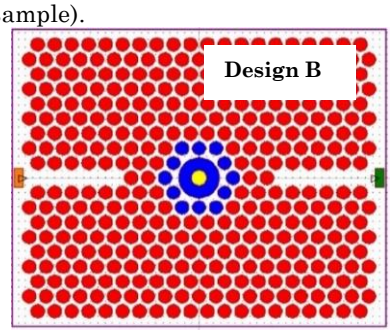

Fig. 6 – Schematic of the second proposed 2D-PhC biosensor

Simulations are performed and the designed biosensor provides good accuracy and transmission. We can notice that the sensitivity increases by increasing the number of functionalized holes. A high sensitivity of more than 650 nm/RIU, an ultra-high-quality factor (Q-factor) of up to 10^5 giving a sensor figure of merit (FOM) of up to 10^4 RIU^{-1}, and a low detection limit of 10^{-6} RIU can be achieved for the proposed design. The normalized transmission reaches 94 %, which proves that the total transmission loss of the proposed biosensor is quite small.

4.3 The Third Proposed Design (Design C)

To further enhance the sensitivity of the biosensor, the third design is proposed (Design C) in Fig. 7, the analyte is infiltrated into all the air holes around the ring-shaped cavity area (holes in blue color), the infiltration of all holes has a significant effect on the performance of the biosensor.

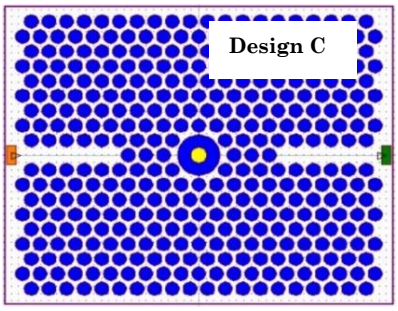

Fig. 7 – Schematic of the third proposed 2D-PhC biosensor

Fig. 8 illustrates the normalized transmission spectra for the third design (Design C) for different refractive in-dices. The normalized transmission spectrum is shifted with the change of the refractive index from healthy to an infected one. The curves shift towards higher wavelengths with the increase of refractive indices.

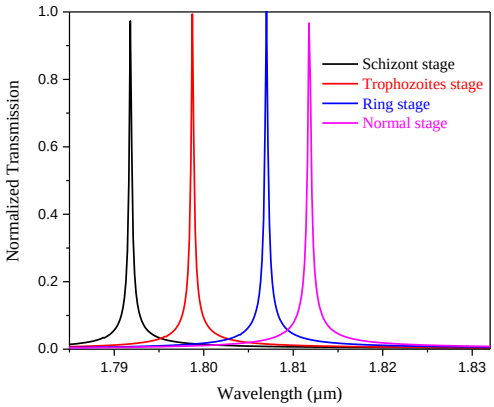

Fig. 8 – Normalized transmission spectrum for the third proposed design at optimized parameters $R_{in} = 0.23$ and $R_{out} = 1.2a$

As expected, the achieved results of the third design for different malaria stages show that the sensitivity and the normalized transmission are improved by increasing the number of functionalized holes, the sensitivity is improved and reaches the highest value of 702.73 nm/RIU for $n = 1.373$ (Schizont stage), and a high value of transmission of 99.9 % was achieved for $n = 1.395$ (Ring stage). However, the Q-factor and DL are significantly reduced as a result of the quantity of reflections inside the device [19].

As illustrated in Fig. 9, according to the fitting curves, a good linear relationship between the resonant wavelength and the refractive index of the analyte has been observed for the three designs (Designs A, B, C).

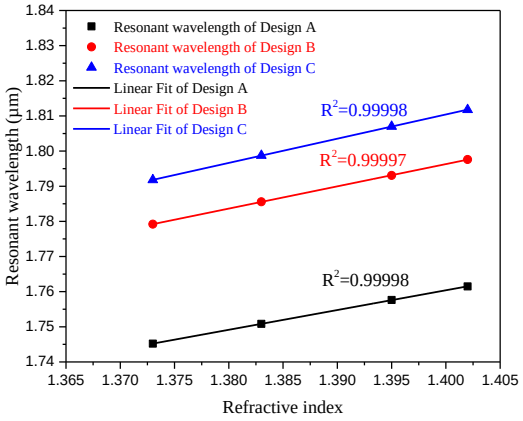

Fig. 9 – Relationships between the refractive index and the resonant wavelengths for designs (A, B, and C)

The proposed biosensor has high linearity according to the correlation coefficient R^2, which is equal to 0.99998, 0.99997, and 0.99998 for designs A, B, and C, respectively. This proves the effectiveness of the proposed designs for the detection of malaria disease. As it is well known that a high linear fitting property is an important indicator of a good sensor.

To compare our findings with previous studies related to the different stages of malaria sensing, Table 2 is presented. The obtained results reflect that our proposed biosensor possesses a high sensitivity of 702.73 nm/RIU, for the change in refractive index, an extremely high Q-factor up to 10^6 giving a very low detection limit of 10^{-7}.

5. CONCLUSIONS

In this work, we have proposed a novel 2D-PhC platform for the diagnosis of malaria disease. We have enhanced the sensitivity by increasing the sensing area; the number of functionalized holes plays a crucial role in the augmentation of the sensitivity and the normalized transmission. Moreover, designs B and C are created by modifying the region filled with the RBCs to enhance the device sensitivity. The simulations are carried out by changing the refractive index of the analyte and our findings have revealed a high sensitivity $S = 702.73$ nm/RIU, a high Q-factor up to 10^6, an ultra-high FOM of 10^6 RIU^{-1}, and a low detection limit of 10^{-7}. The proposed device has ultra-compact size of 9.78×8.84 μm^2 and shows good results for the effective diagnosis of malaria-infected RBCs at an early stage.

Table 2 – Comparison of related photonic crystal biosensors for malaria diagnosis with our proposed biosensor

References	Refractive index		S (nm/RIU)	Q-factor	DL (RIU)	Year
[12]	1.371		*	1.99×10^5	*	2021
	1.381		*	2×10^5	*	
	1.396		*	2.02×10^5	*	
	1.408		495.73	2.03×10^5	8.07×10^{-6}	
[3]	1st design	1.373	355.8953	152.513	*	2021
		1.383	356.4207	148.0285	*	
		1.395	356.9152	142.883	*	
		1.399	357.2168	142.2426	*	
[20]	2nd design	1.373	427.18	5974.80	*	2020
		1.383	416.27	5390	*	
		1.395	406.13	5978.36	*	
		1.402	401.44	7187.27	*	
Our proposed biosensor	1st design	1.373	578.08	1.7548×10^6	1.72×10^{-7}	—
		1.383	576.50	2.0747×10^6	1.46×10^{-7}	
		1.395	574.94	1.7652×10^6	1.73×10^{-7}	
		1.402	573.43	1.1956×10^6	2.56×10^{-7}	
	2nd design	1.373	652.05	1.7503×10^5	1.55×10^{-6}	
		1.383	650.12	1.2370×10^5	2.22×10^{-6}	
		1.395	647.15	1.4663×10^5	1.88×10^{-6}	
		1.402	646.96	1.4759×10^5	1.88×10^{-6}	
	3rd design	1.37	702.73	3288	7.75×10^{-5}	
		1.383	701.56	3121.6	8.21×10^{-5}	
		1.395	700.21	3247.6	7.94×10^{-5}	
		1.402	698.72	2985.9	8.68×10^{-5}	

*Not available

REFERENCES

1. Y. Lo, Y.W. Cheung, L.Wang, M.Lee, G.Figueroa-Miranda, S.Liang, D.Mayer, J.A.Tanner, *Biosens. Bioelectron.* **192**, 113472 (2021).
2. WHO, "Malaria".
3. A. Rashidnia, H. Pakarzadeh, M. Hatami, *Opt Quant Electron*. **54**, 38 (2022).
4. WHO, "World malaria report 2020: 20 years of global progress and challenges," (2020).
5. G. Dutta, *Mater. Sci. Energy Technol.* **3**, 150 (2020).
6. H. Tayoub, A. Hocini, A. Harhouz, *J. Nano- Electron. Phys.* **13** No 6, 06005 (2021).
7. A. Harhouz, A. Hocini, H. Tayoub, *Telematique*, **21**, 1 (2023).
8. T. Zouache, A. Hocini, X. Wang, *Optik* **172**, 97 (2018).
9. N.A. Mohammed, M.M. Hamed, A.A.M. Khalaf, S. EL-Rabaie, *Eur. Phys. J. Plus*, **135**, 11 (2020).
10. V. Sharma, V.L. Kalyani, *Int. J. Emerg. Res. Manag. Technol.* **6**, 6 (2018).
11. S. Bendib, C. Bendib, *J. Biosens. Bioelectron.* **9** No 3, 1000257 (2018).
12. Ankita, B. Suthar, A. Bhargava, *Plasmonics* **16**, 59 (2021).
13. M.T. Tammam, Z.A. Zaky, A. Sharma, Z.S. Matar, A.H. Aly, M.A. Mohaseb, *IOP Conf. Ser. Mater. Sci. Eng.* **1171**, 012005 (2021).
14. H. Tayoub, A. Hocini, A. Harhouz, *Instrum. Mes. Métrologie*, **18**, 165 (2019).
15. S. Jindal, S. Sobti, M. Kumar, S. Sharma, M.K. Pal, *IEEE Sens. J.* **16** No 10, 3705 (2016).
16. K.V. Ragavan, S. Kumar, S. Swaraj, S. Neethirajan, *Biosens. Bioelectron.* **105**, 188 (2018).
17. A. Harhouz, A. Hocini,H. Tayoub, *IOP Conf. Ser. Mater. Sci. Eng.* **1046**, 012001 (2021).
18. S. Arafa, M. Bouchemat, T. Bouchemat, A. Benmerkhi, A. Hocini, *Opt. Commun.* **384**, 93 (2017).
19. M.A. Butt, S.N. Khonina, N.L. Kazanskiy, *Optik* **202**, 163655 (2020).
20. M. Franky, J. Molina-Franky, L. Cuy-Chaparro, A. Camargo, C. Reyes, M. Gómez, D. Ricardo Salamanca, M. Alfonso Patarroyo, M. Elkin Patarroyo, *Malar. J.* **19**, 56 (2020).

Високоефективний двовимірний фотонно-кристалічний біосенсор для діагностики еритроцитів, інфікованих малярією

H. Tayoub[1,2], A. Hocini[1], A. Harhouz[1]

[1] *Laboratoire d'Analyse des Signaux et Systèmes, Department of Electronics, University of M'Sila BP.166, Route Ichebilia, 28000 M'Sila, Algeria*
[2] *Research Center in Industrial Technologies CRTI, P.O.BOX :64, Cheraga, 16014 Algiers, Algeria*

У статті запропоновано двовимірний фотонно-кристалічний біосенсор на основі кільцевої порожнини. Він призначений для діагностики уражених малярією еритроцитів в діапазоні довжин хвиль 1130-1860 нм для ТМ-поляризованого світла. Пропонований біосенсор складається з двох хвилеводів, з'єднаних з однією кільцеподібною мікропорожниною, яку отримано видаленням семи отворів решітки, причому мікропорожнина відокремлена від двох хвилеводів трьома отворами. Проникнення аналіту в кільцеподібну порожнину змінює її показник заломлення, і ця зміна показника заломлення інфікованих і нормальних (неінфікованих) еритроцитів викликає відповідний зсув довжини хвилі на вихідному терміналі. Робочими параметрами біосенсора є висока чутливість понад 700 нм/RIU, коефіцієнт надвисокої якості (Q-фактор) до 10^6, що дає добротність датчика до 10^6 RIU^{-1}, і низька межа виявлення 10^{-7} RIU. Пропонований пристрій також має ультра-компактний розмір 9,78×8,84 мкм^2, що робить його привабливим для застосування в мікросхеміах. Отримані результати показали, що кільцеподібна конфігурація отворів забезпечує оптичне обмеження в області порожнини. Запропонована конструкція моделюється за допомогою методу розширення плоскої хвилі (PWE) і алгоритму кінцевої різниці в часовій області (FDTD).

Ключові слова: Фотонний кристал, Кільцеподібна порожнина, Біосенсор, Малярія, Чутливість, Добротність.